

Exploring the Potential of Mesoporous Silica, SBA-15, as an Adsorbent for Light Hydrocarbon Separation

Bharat L. Newalkar,[†] Nettem V. Choudary,^{‡,§} Prakash Kumar,[‡] S. Komarneni,^{*,†,||} and Thirumaleshwara S. G. Bhat^{*,‡,⊥}

Materials Research Laboratory, Materials Research Institute, The Pennsylvania State University, University Park, Pennsylvania 16802, and Research Centre, Indian Petrochemicals Corporation Limited, Vadodara 391 346, India

Received June 29, 2001. Revised Manuscript Received October 23, 2001

Equilibrium adsorption isotherms for methane, ethane, ethylene, acetylene, propane, and propylene have been measured for the first time on mesoporous silica, SBA-15, and the data are analyzed by using the Langmuir–Freundlich adsorption isotherm model. The adsorption capacities for ethylene and propylene are found to be higher than those for corresponding alkanes. Likewise, adsorption of acetylene is more pronounced as compared to ethylene. The *isosteric* heats of adsorption for various adsorbates estimated by the Clausius–Clapeyron equation are higher for olefins and acetylene and are comparable with those reported for π -complexation based systems. Such a trend has in turn suggested a higher affinity of SBA-15 framework for alkenes over corresponding alkanes, which has been examined in terms of the textural characteristics of SBA-15. It is suggested that SBA-15 can potentially be a good adsorbent for separation of light hydrocarbons.

Introduction

The synthesis of ordered mesoporous materials in 1992 sparked worldwide interest in the field of heterogeneous catalysis and separation science.¹ However, the poor hydrothermal stability of such materials has restricted their applications. This placed an emphasis on the search for new structures with new framework compositions, which recently resulted in the synthesis of ordered, hydrothermally stable mesoporous silica, SBA-15,² thus providing an opportunity for the development of a wide range of applications in the fields of adsorption, catalysis, and advanced materials.^{3–8} Ap-

plications such as heavy metal remediation, sequestration, and controlled release of proteins have been developed by surface modification of the SBA-15 framework via bonding of organosilanes.^{8–14} It has also been found to be applicable as a waveguide and a mirrorless laser.¹⁵ Such a wide range of applications has also provided new synthetic opportunities to obtain these materials in various meso- and macroscopic forms.¹⁶ Furthermore, it has been successfully employed in the preparation of mesoporous carbon and metal nanowires, nanoballs, and nanocables by using the guest–host approach.^{17–20}

* To whom correspondence should be addressed.

† The Pennsylvania State University.

‡ Indian Petrochemicals Corporation Limited.

§ Present address: Corporate R&D, Bharat Petroleum Corporation Limited, Plot 2A, Udyog Kendra, Greater Noida, India.

|| Tel: 1-814-865-1542. Fax: 1-814-865-2326. E-mail: komarneni@psu.edu.

⊥ Tel: 011-91-265-262011 ext: 3673. Fax: 011-91-265-262098.

E-mail: sgtbhat@ipclmail.com.

(1) (a) Kresge, C. T.; Leonowicz, M. E.; Roth, W. J.; Vartuli, J. C.; Beck, J. S. *Nature* **1992**, *359*, 710. (b) Beck, J. S.; Vartuli, J. C.; Roth, W. J.; Leonowicz, M. E.; Kresge, C. T. *J. Am. Chem. Soc.* **1992**, *114*, 10834. (c) Chenite, A.; Page, Y. L. *Chem. Mater.* **1995**, *7*, 1015.

(2) (a) Zhao, D.; Feng, J.; Huo, Q.; Melosh, N.; Fredrickson, G. H.; Chmelka, B. F.; Stucky, G. D. *Science* **1998**, *279*, 548. (b) Zhao, D.; Huo, Q.; Feng, J.; Chmelka B. F.; Stucky, G. D. *J. Am. Chem. Soc.* **1998**, *120*, 6024.

(3) Luan, Z.; Maes, E. M.; van der Heide, P. A. W.; Zhao, D.; Czernuszewicz, R. S.; Keven, L. *Chem. Mater.* **1999**, *11*, 3680.

(4) Cheng, M.; Wang, Z.; Sakurai, K.; Kumata, F.; Saito, T.; Komatsu, T.; Yashima, T. *Chem. Lett.* **1999**, *131*.

(5) Yue, Y.; Gedeon, A.; Bonardet, J.-L.; Melosh, N.; D'Espinose, J.-B.; Fraissard, J. *Chem. Commun.* **1999**, 1967.

(6) (a) Luan, Z.; Hartmann, M.; Zhao, D.; Zhou, W.; Kevan, L. *Chem. Mater.* **1999**, *11*, 1621. (b) Newalkar, B. L.; Olanrewaju, J.; Komarneni, S. *Chem. Mater.* **2001**, *13*, 552.

(7) Morey, M. S.; O'Brien, S.; Schwarz, S.; Stucky, G. D. *Chem. Mater.* **2000**, *12*, 898.

(8) Luan, Z.; Bae, J. Y.; Kevan, L. *Chem. Mater.* **2000**, *12*, 3202.

(9) (a) Bae, S. J.; Kim, S.-W.; Hyeon, T.; Kim, B. M. *Chem. Commun.* **1999**, *31*. (b) Park, M.; Komarneni, S. *Microporous Mesoporous Mater.* **1998**, *25*, 75.

(10) Liu, A. M.; Hidajat, K.; Kawi, S.; Zhao, D. Y. *Chem. Commun.* **2000**, *1145*.

(11) Han, Y.-J.; Stucky, G. D.; Butler, A. *J. Am. Chem. Soc.* **1999**, *121*, 9897.

(12) Lin, H.-P.; Yang, L.-Y.; Mou, C.-Y.; Liu, S.-B.; Lee, H.-K. *New J. Chem.* **2000**, *24*, 253.

(13) Margolese, D.; Melero, J. A.; Christiansen, S. C.; Chmelka, B. F.; Stucky, G. D. *Chem. Mater.* **2000**, *12*, 2448.

(14) Markowitz, M. A.; Klaehn, J.; Hendet, R. A.; Qadriq, S. B.; Golledge, S. L.; Castner, D. G.; Gaber, B. P. *J. Phys. Chem. B* **2000**, *104*, 10820.

(15) Yang, P.; Wirnsberger, G.; Huang, H. C.; Cordero, S. R.; McGehee, M. D.; Scott, B.; Deng, T.; Whitesides, G. M.; Chmelka, B. F.; Buratto, S. K.; Stucky, G. D. *Science* **2000**, *287*, 465.

(16) (a) Lu, Y.; Ganguli, R.; Drewien, C. A.; Anderson, M. T.; Brinker, C. J.; Gong, W.; Guo, Y.; Soyez, H.; Dunn, B.; Huang, M. H.; Zink, J. I. *Nature* **1997**, *389*, 364. (b) Ogawa, M.; Igarashi, T.; Kuroda, K. *Bull. Chem. Soc. Jpn.* **1997**, *70*, 2833. (c) Zhao, D.; Yang, P.; Melosh, N.; Feng, J.; Chmelka, B. F.; Stucky, G. D. *Adv. Mater.* **1998**, *10*, 1380. (d) Tolbert, S. H.; Firouzi; Stucky, G. D.; Chmelka, B. F. *Science* **1997**, *278*, 264. (e) Attard, G. S.; Glyde, J. C.; Göltner, C. G. *Nature* **1995**, *378*, 366. (f) Feng, P.; Bu, X.; Stucky, G. D.; Pine, D. J. *J. Am. Chem. Soc.* **2000**, *122*, 994.

(17) Shinae Jun, S.; Joo, S. H.; Ryoo, R.; Kruk, M.; Jaroniec, M.; Liu, Z.; Ohsuna, T.; Terasaki, O. *J. Am. Chem. Soc.* **2000**, *122*, 10712.

(18) Han, Y.-J.; Kim, J. M.; Stucky, G. D. *Chem. Mater.* **2000**, *12*, 2068.

In comparison to these efforts, no attempt has been made so far, to the best of our knowledge, to understand and explore the potential use of SBA-15 as an adsorbent with it especially pertaining to the separation of hydrocarbons. Therefore, the main objective of the present study is to investigate the adsorption properties of SBA-15 with a view to understand its usefulness as an adsorbent for commercially important light hydrocarbon separation, particularly C_2 and C_3 hydrocarbons. Thus, equilibrium adsorption isotherms for methane, ethane, ethylene, acetylene, propane, and propylene were measured by using the volumetric adsorption measurement technique at 30 and 50 °C and the data were analyzed using various models. The *isosteric* heat of adsorption, adsorption capacity, and selectivities were estimated to be able to learn about the usefulness of mesoporous silica SBA-15 as an adsorbent for the separation of hydrocarbons.

Experimental Section

Sample Preparation. Siliceous SBA-15 sample was prepared by templating tetraethyl orthosilicate, TEOS, (Aldrich) with a triblock poly(ethyleneoxide)-poly(propylene oxide)-poly(ethylene oxide) ($EO_{20}PO_{70}EO_{20}$, $M_w = 5800$, Aldrich) under microwave-hydrothermal conditions as described elsewhere.²¹ The crystallized product was filtered, washed with warm distilled water, dried at 110 °C, and finally calcined at 540 °C in air for 6 h. The thus-obtained sample was subjected to characterization.

Characterization. X-ray diffraction patterns were recorded by using a Philips X'pert powder diffractometer system with $Cu K\alpha$ radiation, a 0.02° step size, and 1 s step time over the range $0.5^\circ < 2\theta < 6^\circ$.

The textural properties of the samples were evaluated by using nitrogen adsorption/desorption measurements with an Autosorb-1 (Quantachrome) unit. Nitrogen adsorption/desorption isotherms were measured at -196 °C after degassing the samples below 10^{-3} Torr at 200 °C for 4 h. The BET specific surface area (S_{BET}) was estimated by using adsorption data in a relative pressure range from 0.04 to 0.2. The external surface area, S_{ex} , total surface area, S_t , primary mesopore surface area, S_p , micropore volume, V_{mi} , and primary mesopore volume, V_p , were estimated by using the α_s -plot method, as described elsewhere.^{22,23} *Amorphous nonporous silica* ($S_{BET} = 7.0$ m^2/g , Thikol) was used as a reference adsorbent. The calculation of mesopore size distribution (PSD) was performed by analyzing the adsorption data of N_2 isotherm with the use of the recently developed KJS (Kruk, Jaroniec, Sayari) approach.²⁴ The pore diameter corresponding to the maximum of PSD is denoted as W_{KJS} . The total pore volume, V_t , was estimated from the amount adsorbed at a relative pressure of 0.95.

Adsorption Isotherms Measurements. Adsorption isotherms for methane, ethane, ethylene, acetylene, propane, and propylene were measured by using volumetric adsorption measurement unit at 30 and 50 °C. Typically, about 1 gm of activated sample was loaded in a volumetric adsorption unit, which was fitted with two MKS absolute pressure transducers model 122AA (100 and 1000 mmHg range, 0.01 and 0.1 mmHg accuracy, respectively). The sample temperature was maintained at 0.01 °C by using a JULABO F10 thermostatic

Table 1. Textural Parameters of the SBA-15 Sample

a_0^a , W_{KJS} , V_t at $p/P = 0.95$, cc/g	V_p , cc/g	V_{mi} , cc/g	S_{BET} , m^2/g	S_t , m^2/g	S_{ex} , m^2/g	S_p^b , m^2/g	(W_{KJS}/V_p)
105 73	0.97	0.88	0.04	791	812	24.4	788 6.53

^a $a_0 = 2d_{100}/\sqrt{3}$. ^b $S_p = S_t - S_{ex}$.

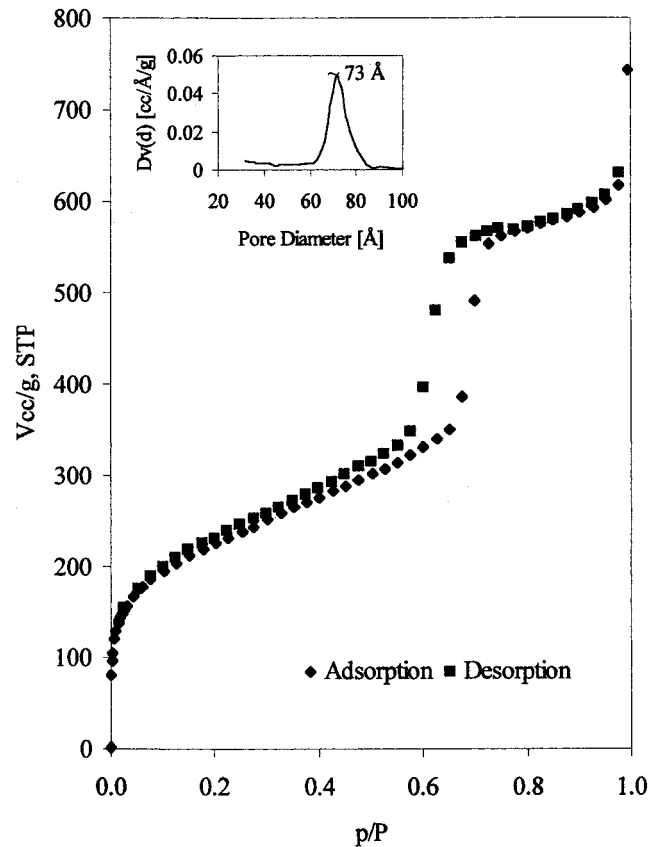


Figure 1. Nitrogen adsorption/desorption isotherm for SBA-15 sample obtained under microwave-hydrothermal conditions at -196 °C. (An inset shows a pore size distribution for the sample based on KJS approach).

circulating bath. All the adsorbates used in the present study were of UHP grade (purity $> 99.99\%$). At the end of the adsorption run, a desorption experiment was performed to check the reversibility of the adsorption isotherm. All the measurements were performed in duplicate to ensure the quality as well as reproducibility of the data. The measured adsorption data were analyzed by using the Langmuir-Freundlich adsorption isotherm model.

Results and Discussion

Adsorbent Characterization. The calcined SBA-15 sample displayed a well-resolved pattern with a sharp peak in the range of about 0.8° and two long order weak peaks in the range of about 1.6 and 1.7° which is in agreement with the reported pattern.^{2b} The XRD peaks are indexed to a hexagonal lattice with $d(100)$ spacing corresponding to a large unit cell parameter a_0 (Table 1). Typical nitrogen adsorption/desorption isotherms for the SBA-15 sample (measured at -196 °C) and pore size distribution are shown in Figure 1. The nitrogen adsorption/desorption isotherms are found to be of type IV in nature as per the IUPAC classification and exhibited a H1 hysteresis loop, which is typical of mesoporous solids.²³ The estimated textural parameters such as specific surface area S_{BET} , total surface area,

(19) Kang, H.; Jun, Y.-W.; Park, J.; Lee, K.-B.; Cheon, J. *Chem. Mater.* **2000**, *12*, 3530.

(20) Jang, J. S.; Lim, B.; Lee, J.; Hyeon, T. *Chem. Commun.* **2001**, 83.

(21) Newalkar, B. L.; Komarneni, S.; Katsuki, H. *Chem. Commun.* **2000**, 2389.

(22) Gregg, S. J.; Sing, K. S. W. *Adsorption, Surface Area and Porosity*; Academic Press: New York, 1982.

(23) Sayari, A.; Liu, P.; Kruk, M.; Jaroniec, M. *Langmuir* **1997**, *13*, 2499.

(24) Kruk, M.; Jaroniec, M.; Sayari, A. *Langmuir* **1997**, *13*, 6267.

Table 2. Isosteric Heats (ΔH) of Adsorption at Low Coverage, Equilibrium Adsorption Capacities (Q) at 1 atm, and Fitted Langmuir–Freundlich Constants (V_m , b , and n) for Various Hydrocarbons on Mesoporous Silica SBA-15

adsorbate	ΔH , kJ/mol	t , °C	Q , mmol/g	V_m , mmol/g	$b \times 10^3$, mm Hg ⁻¹	n
methane (H ₄)	2.0	30	0.11	1.44	0.08	1.04
		50	0.09	2.31	0.09	0.92
ethane (C ₂ H ₆)	5.9	30	0.56	2.72	0.75	0.88
		50	0.38	2.62	0.45	0.89
ethylene (C ₂ H ₄)	8.4	30	0.89	2.91	1.69	0.84
		50	0.60	2.36	0.90	0.89
acetylene (C ₂ H ₂)	9.8	30	1.55	4.15	4.22	0.75
		50	1.11	3.41	2.24	0.81
propane (C ₃ H ₈)	9.2	30	1.24	4.72	2.88	0.73
		50	0.87	3.47	1.65	0.80
propylene (C ₃ H ₆)	14.8	30	1.94	4.90	11.08	0.61
		50	1.40	3.91	4.99	0.71

Table 3. Selectivity Ratio (Ratio of Pure Gas Adsorption Capacity) at 1 atm for Various Hydrocarbon Gases on Mesoporous Silica SBA-15

system	adsorption selectivity ratio at 1 atm	
	30 °C	50 °C
ethane/methane	4.9	4.3
ethylene/ethane	1.6	1.6
propylene/propane	1.6	1.6
acetylene/ethylene	1.8	1.9
propane/ethane	2.2	2.3
propylene/ethylene	2.2	2.3

S_t , external surface area, S_{ex} , primary mesopore volume, V_p , micropore volume, V_{mi} , total pore volume, V_p , and mesopore size, W_{KJS} , are compiled in Table 1. The obtained results confirmed the structural as well as the adsorption crystallinity of the adsorbent.

Adsorption Isotherms of C₂ and C₃ Hydrocarbons. Figure 2 depicts the adsorption isotherms for various adsorbates measured at 30 and 50 °C, respectively. The equilibrium adsorption capacities for various hydrocarbons at 1 atm are compiled in Table 2. The isotherms showed that the adsorption capacity for unsaturated hydrocarbons is substantially higher than the corresponding paraffin. For example, at 30 °C and 1 atm, 1.94 mmol/g of propylene was adsorbed as compared to 1.24 mmol/g of propane. The following trend in adsorption capacity was observed for various hydrocarbons: propylene > acetylene > propane > ethylene > ethane > methane. Further, the rise in the adsorption capacity with pressure was higher for olefins compared to that for the corresponding paraffin. Such behavior was more pronounced in the case of the C₃ hydrocarbons; that is, the increase in adsorption capacity is much higher for propylene than for propane with pressure. Because of the nonpolar nature of the adsorbent surface, this may be ascribed to the higher quadrupole moment of olefin molecules over corresponding paraffins. The adsorption capacities for propylene and propane on SBA-15 are comparable to those reported for silica gel.²⁵ The pure-component adsorption ratios for ethane over methane and propane over ethane at 30 °C and 1 atm are observed to be 4.9 and 2.2, respectively (Table 3). Furthermore, adsorption capacity ratios for propylene/propane and ethylene/ethane are found to be about 1.6. The pure-component adsorption ratio for propylene over ethylene is about 2.2 at 30 °C. On the other hand, adsorption of acetylene is favored over ethylene by a ratio of about 1.8.

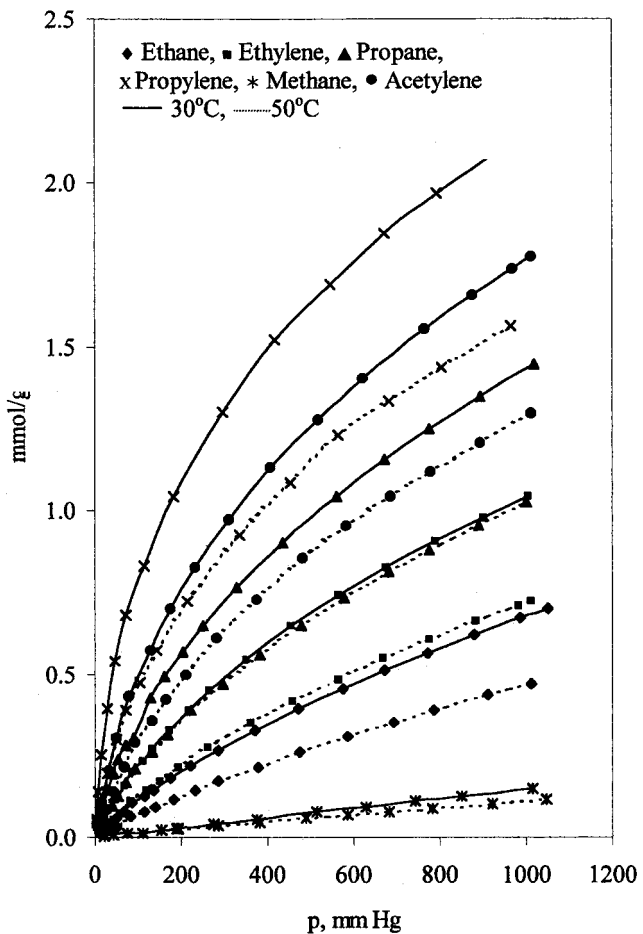


Figure 2. Equilibrium adsorption isotherms for various hydrocarbons on SBA-15 at 30 and 50 °C.

Evaluation of Equilibrium Isotherm Model. The adsorption data were analyzed with the use of Langmuir and Langmuir–Freundlich models by nonlinear regression approach. The experimental data were well represented by the Langmuir–Freundlich adsorption isotherm model, that is, $V = V_m bp^n / (1 + bp^n)$ where V and V_m are the amounts adsorbed at equilibrium pressure p in mmHg and monolayer adsorption capacity in mmol/g and b and n are Langmuir and Freundlich constants, respectively. The equilibrium adsorption parameters so obtained are also compiled in Table 2. It can be seen that the Langmuir–Freundlich constants b , which is a measure of interaction between adsorbate and adsorbent, of unsaturated hydrocarbons are higher than those of saturated ones, thus suggesting a stronger interaction of former molecules with the adsorbent surface.

Isosteric Heats of Adsorption. The isosteric heats of adsorption (ΔH) for various adsorbates are estimated by using the Clausius–Clapeyron equation (Table 2), and their dependence on adsorption coverage is shown in Figure 3. The heats of adsorption for propylene, propane, ethylene, ethane, methane, and acetylene were 14.8, 9.2, 8.4, 5.9, 2.0, and 9.8 kJ/mol, respectively. The isosteric heats of adsorption are found to be higher for ethylene and propylene when compared to ethane and propane, respectively, over the entire adsorption coverage. The heats of adsorption of acetylene are higher than those obtained for ethylene. Furthermore, a sharp drop in the heats of adsorption is noticed for unsaturated

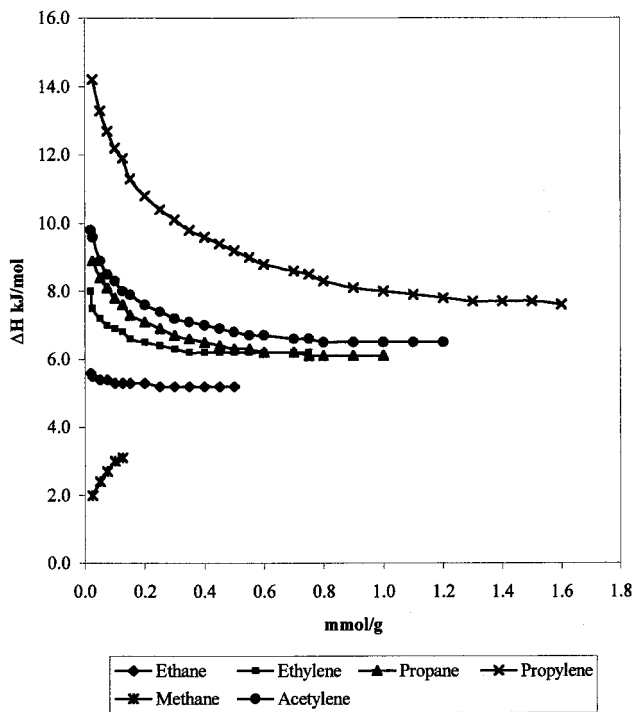


Figure 3. Dependence of isosteric heats of adsorption for C_1 , C_2 , and C_3 hydrocarbons on SBA-15 with coverage.

hydrocarbons, particularly for propylene, with an increase in adsorption coverage. Heats of adsorption for propylene on SBA-15 are also found to be higher than those reported for silica gel.²⁵ The dependence of heats of adsorption of ethane and methane on adsorption coverage is not significant. High heats of adsorption observed for unsaturated hydrocarbons, particularly for propylene, reflected the presence of surface heterogeneity in the form of specific adsorption sites for these molecules in the SBA-15 framework. The presence of specific adsorption sites is explained below on the basis of textural characteristics of the adsorbent.

Origin of Specific Adsorption Sites. Recently reported structural elucidation studies on SBA-15 indicated the existence of micropores within the pore walls of its mesopores.²⁶ The origin of such micropores is ascribed to the hydrophilic nature of poly(ethylene oxide) (PEO) blocks of the template that are expected to be deeply occluded within the silica walls, which, upon calcination, are responsible for the generation of microporosity.²⁶ Such deep occlusion of EO blocks has also been confirmed by means of NMR investigations.²⁷ Furthermore, quantitative measurements by X-ray diffraction have shown the existence of microporous corona around the mesopores of SBA-15 as a result of such occlusion.²⁶ In view of these aspects, the SBA-15 framework is visualized as a complex network consisting of an array of mesopore–micropore networks instead of an array of uniform mesoporous networks like other

ordered mesoporous silica such as MCM-41. The complexity of the SBA-15 framework has also been confirmed on the basis of the detailed nitrogen adsorption–desorption measurements wherein it is found to exhibit a relation between the pore size, pore volume, and specific surface area ($WS/V = 5.8–10.8$, where W , S , and V are the mesopore size, mesopore surface area, and mesopore volume, respectively), which is significantly different from that for circular or hexagonal pores of MCM-41 type of material ($WS/V = 4.0–4.4$).²⁸

The presence of micropores in the sample used in the present adsorption studies is confirmed by the α_s -plot (Table 1). The presence of micropores is further reinforced by the relation between mesopore size, surface area, and volume ($WS/V = 6.5$, Table 1). Thus, we believe that adsorption sites are in the form of these micropores. So, adsorbate molecules are transported to these sites through *mesopores* where they are expected to adsorb strongly. Additional support for the proposed adsorption sites can be obtained by performing the adsorption studies on SBA-15 samples with controlled porosity. Recently, both postsynthesis and *in situ* synthesis methodologies have been proposed to achieve control over the microporosity of the SBA-15 framework.^{28,29} Currently, we are investigating these aspects in detail.

Adsorption Selectivity. The higher adsorption capacities and heats of adsorption observed for unsaturated hydrocarbons as compared to corresponding alkanes indicate a possibility of SBA-15 acting as a medium for adsorptive separation of the hydrocarbon mixtures. In fact, for the last 50 years, these separations have continued to be accomplished through cryogenic processes (distillations) which are very energy intensive due to close relative volatilities.³⁰ Therefore, many alternatives are being investigated^{31,32,33,34–39} all over the world to achieve this separation, among which

(28) Ryoo, R.; Ko, C. H.; Kruk, M.; Antochshuk, V.; Jaroniec, M. *J. Phys. Chem. B* **2000**, *104*, 11465.

(29) (a) Miyazawa, K.; Inagaki, S. *Chem. Commun.* **2000**, 2121. (b) Newalkar, B. L.; Komarneni, S. *Chem. Mater.* **2001**, *13*, 4573.

(30) Meyers, R. A. *Handbook of Petroleum Refining Process*; McGraw-Hill: New York, 1997.

(31) Eldridge, R. B. *Ind. Eng. Chem. Res.* **1993**, *32*, 2208.

(32) (a) King, C. J. *Handbook of Separation Process Technology*; Rousseau, R. W., Ed.; Wiley-Interscience: New York, 1987. (b) Yang, R. T.; Kikkilides, E. S. *AIChE J.* **1995**, *41*, 509. (c) Wu, Z.; Han, S. S.; Cho, S. H.; Kim, J. N.; Chue, K. T.; Yang, R. T. *Ind. Eng. Chem. Res.* **1997**, *36*, 2749. (d) Padin, J.; Yang, R. T.; Munson, C. L. *Ind. Eng. Chem. Res.* **1999**, *38*, 3614. (e) Cheng, L. S.; Yang, R. T. *Adsorption* **1995**, *1*, 61. (f) Quinn, H. W. *Prog. Sep. Purif.* **1971**, *4*, 133. (g) Ho, W. S.; Doyle, G.; Savage, D. W.; Pruitt, R. L. *Ind. Eng. Chem. Res.* **1988**, *27*, 334. (h) Blytas, G. C. *Separation and Purification Technology*; Li, N. N.; Calo, J. M., Eds.; Marcel Dekker: New York, 1992. (i) Padin, J.; Yang, R. T. *Chem. Eng. Sci.* **2000**, *55*, 2607.

(33) (a) Yang, R. T.; Foldes, R. *Ind. Eng. Chem. Res.* **1996**, *35*, 1006.

(b) Padin, J.; Yang, R. T. *Ind. Eng. Chem. Res.* **1997**, *36*, 4224. (c) Kodde, A. J.; Padin, J.; van der Meer, P. J.; Mittelmeijer-Hazeleger, M. C.; Bliek, A.; Yang, R. T. *Ind. Eng. Chem. Res.* **2000**, *39*, 3108.

(34) Cho, S. H.; Han, S. S.; Kim, J. N.; Chue, T. K.; Choudary, N. V.; Kumar, P. Korean Patent No. 0279881, Nov 06, 2000.

(35) Cho, S. H.; Han, S. S.; Kim, J. N.; Choudary, N. V.; Kumar, P. Indian Patent Application No. IP/915/Del/99, June 25, 1999.

(36) Cho, S. H.; Han, S. S.; Kim, J. N.; Kumar, P.; Choudary, N. V.; Bhat, S. G. T. Indian Patent Application No. IP/1289/Del/99, Sept 23, 1999.

(37) Cho, S. H.; Han, S. S.; Kim, J. N.; Chue, T. K.; Choudary, N. V.; Kumar, P. U.S. Patent Application No. 09/209431, Dec 11, 1998.

(38) Cho, S. H.; Han, S. S.; Kim, J. N.; Kumar, P.; Choudary, N. V.; Bhat, S. G. T. U.S. Patent Application No. 09/411990, Oct 04, 1999.

(39) Cho, S. H.; Han, S. S.; Kim, J. N.; Choudary, N. V.; Kumar, P.; Bhat, S. G. T. In *Proceedings of 8th APCChE Congress*, Seoul, Korea, Aug 16–19, 1999; pp 1777–1780.

(25) (a) Lewis, W. K.; Gilliland, E.; Chertow, B.; Cadogan, W. *Ind. Eng. Chem.* **1950**, *42*, 1319, 1326. (b) Lewis, W. K.; Gilliland, E.; Chertow, B.; Hoffman, W. H. *J. Am. Chem. Soc.* **1950**, *72*, 3. (c) Grande, C. A.; Rodrigues, A. E. *Ind. Eng. Chem. Res.* **2001**, *40*, 1686.

(26) (a) Impérator-Clerc, M.; Davidson, P.; Davidson, A. *J. Am. Chem. Soc.* **2000**, *122*, 11925. (b) Kruk, M.; Jaroniec, M.; Ko, C. H.; Ryoo, R. *Chem. Mater.* **2000**, *12*, 1961.

(27) Melosh, N. A.; Lipic, P.; Bates, F. S.; Wudi, F.; Stucky, G. D.; Fredrickson, G. H.; Chmelka, B. F. *Macromolecules* **1999**, *32*, 4332.

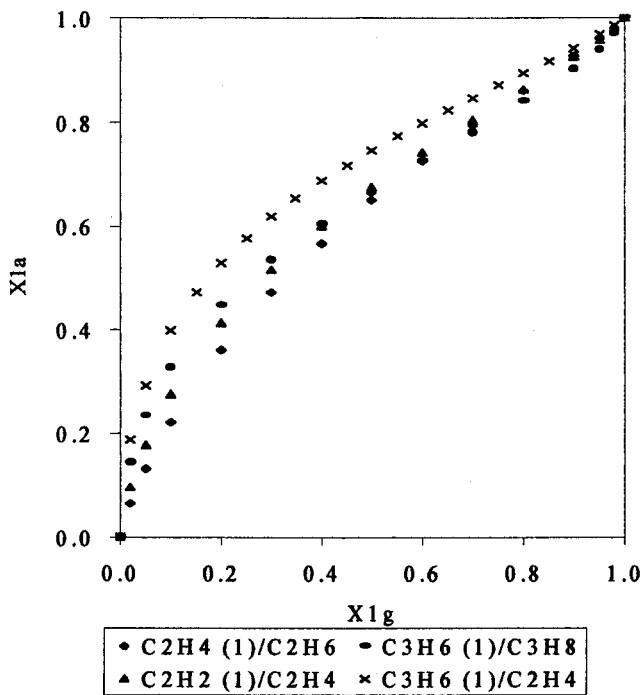


Figure 4. Adsorption isotherms for binary mixtures of C_2 and C_3 hydrocarbons on SBA-15 predicted by the Langmuir–Freundlich (L–F) model at 30 °C. (Suffix 1 is for ethylene (C_2H_4), acetylene (C_2H_2), and propylene (C_3H_6) in binary mixtures: \blacklozenge , C_2H_4/C_2H_6 ; \blacktriangle , C_2H_2/C_2H_4 ; \bullet , C_3H_6/C_3H_8 ; \times , C_3H_6/C_2H_4 . X_1^g and X_1^a are gas and adsorbed phase compositions of ethylene/acetylene/propylene.)

adsorption-based processes are emerging as prominent candidates. The key factor for the commercial viability of the adsorption process is the availability of a selective adsorbent.

To explore the potential of SBA-15 as an adsorbent, we have estimated adsorption selectivities for the binary mixtures of ethane/ethylene, acetylene/ethylene, propane/propylene, and ethylene/propylene by using the extended Langmuir–Freundlich model,^{40a} which is given by $V_i = (V_m)_i b_i p_i^{n_i} / (1 + b_1 p_1^{n_1} + b_2 p_2^{n_2})$, where p_i are partial pressure, b_i are the Langmuir constants, and n_i are Freundlich constants for component i . V_i are the amounts adsorbed from the mixture and $(V_m)_i$ are the monolayer capacities for component i .

Thus, for a two-component (1 and 2) system, the amount of adsorption of each component can be expressed as $V_1 = (V_m)_1 b_1 p_1^{n_1} / (1 + b_1 p_1^{n_1} + b_2 p_2^{n_2})$ and $V_2 = (V_m)_2 b_2 p_2^{n_2} / (1 + b_1 p_1^{n_1} + b_2 p_2^{n_2})$ and the total volume adsorbed can be expressed by $V = V_1 + V_2 = \{(V_m)_1 b_1 p_1^{n_1} + (V_m)_2 b_2 p_2^{n_2}\} / (1 + b_1 p_1^{n_1} + b_2 p_2^{n_2})$. The adsorbed phase composition with respect to component 1 (X_1^a) can also be obtained from the ratio of the amount adsorbed of component 1 to the total volume, that is

$$X_1^a = V_1 / V = (V_m)_1 b_1 p_1^{n_1} / \{(V_m)_1 b_1 p_1^{n_1} + (V_m)_2 b_2 p_2^{n_2}\} = 1 / (1 + ((V_m)_2 b_2 p_2^{n_2} / (V_m)_1 b_1 p_1^{n_1})) \quad (1)$$

On the basis of the above equation, for a given gas-phase composition, X_1^a can be calculated from the values of the L–F constants for the two pure gases. Adsorption

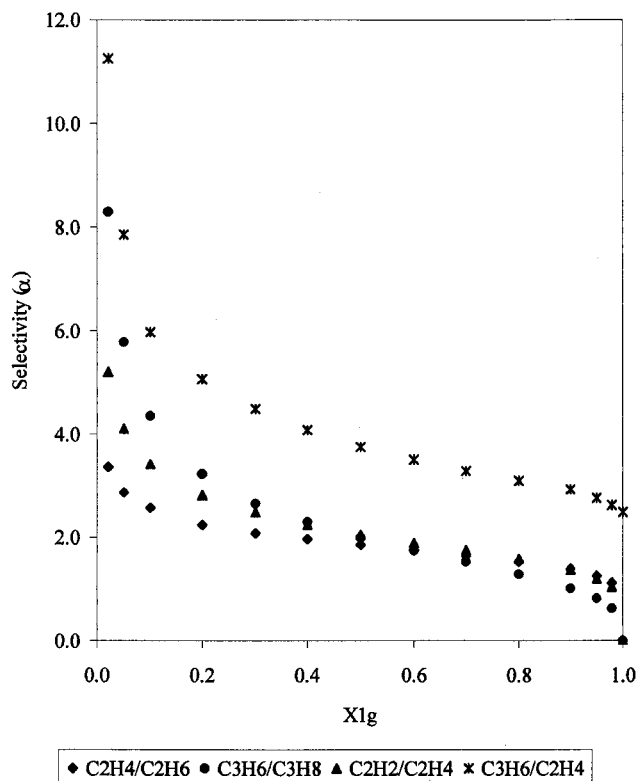


Figure 5. Variation of olefin selectivities (α) as a function of gas-phase composition at 30 °C. (Suffix 1 is for ethylene (C_2H_4), acetylene (C_2H_2), and propylene (C_3H_6) in binary mixtures: \blacklozenge , C_2H_4/C_2H_6 ; \bullet , C_3H_6/C_3H_8 ; \blacktriangle , C_2H_2/C_2H_4 ; \times , C_3H_6/C_2H_4 . X_1^g is the gas-phase composition of ethylene/acetylene/propylene.)

selectivity ($\alpha_{1/2}$) in a binary mixture can also be calculated from adsorbed phase and gas-phase compositions of the two gases by using the relation, $\alpha_{1/2} = X_1^a \cdot X_2^g / X_1^g \cdot X_2^a$.

The predicted adsorbed phase compositions and adsorption selectivities for binary mixtures of ethane/ethylene, acetylene/ethylene, propane/propylene, and ethylene/propylene are shown in Figures 4 and 5, respectively, as a function of gas-phase composition. The results show a high selectivity for propylene over propane and ethylene over ethane. Likewise, the selectivity for the binary mixture of acetylene/ethylene displays high selectivity for acetylene over ethylene. Such a trend is anticipated as the stronger component is expected to dominate in mixture adsorption.^{40b} High adsorption selectivity of olefin at low gas-phase concentration decreases with increase in olefin concentration in the gas phase. Such high selectivity for unsaturated hydrocarbons over corresponding alkanes at low gas-phase concentration makes SBA-15 an attractive adsorbent for olefin enrichment of lean hydrocarbon streams. The average selectivity of about 4 observed for C_2 and C_3 olefins over corresponding alkanes is adequate to be able to design separation processes based on pressure/vacuum swing adsorption principles.⁴¹

Conclusion

Mesoporous silica, SBA-15, shows a reversible uptake of light hydrocarbons and is selective for light alkenes.

(40) (a) Barrer, R. M. *Zeolites and Clay Minerals as Sorbents and Molecular Sieves*; Academic Press: London, 1979. (b) Yang, R. T. *Gas Separation by Adsorption Process*; Butterworth: Boston, 1987.

(41) Jasra, R. V.; Choudary, N. V.; Bhat, S. G. T. *Sep. Sci. Technol.* **1991**, 27, 885.

The adsorption selectivity is ascribed to the presence of micropores in the walls of the SBA-15 framework, which could be tailored. The high adsorption capacity and selectivity for unsaturated hydrocarbons over saturated hydrocarbons shows the potential of SBA-15 as a suitable adsorbent for light hydrocarbon separation.

Acknowledgment. Authors (B.L.N. and S.K.) gratefully acknowledge the support of this work by the NSF MRSEC program under Grant No. DMR-0080019. N.V.C., P.K., and T.S.G.B. are thankful to the management

of Indian Petrochemicals Corporation Limited (IPCL), Vadodara, India for supporting this work. The authors are also thankful to Mr. S. P. Patel, IPCL, India for his assistance during adsorption measurements.

Supporting Information Available: Appendix 1 lists adsorption isotherm data for various hydrocarbons on SBA-15 at 30 and 50 °C; appendix 2 lists nitrogen adsorption data on reference nonporous silica adsorbent (PDF). This material is available free of charge via the Internet at <http://pubs.acs.org>.

CM0106466